Stanford Exploration Project, Report 100, April 20, 1999, pages 35–50

Stanford Exploration Project, Report 100, April 20, 1999, pages 35–50

Preconditioning tau tomography with geologic constraints

Robert G. Clapp and Biondo Biondi[1]

keywords: *preconditioning, regularization, helix, least-squares, tau*

ABSTRACT

Seismic tomography is a non-linear problem with a significant null-space. Our estimation problem often converges slowly, to a geologically unreasonable model, or not at all. One reason for slow or non-convergence is that we are attempting to simultaneously estimate reflector position (mapping velocity) and image our data (focusiing velocity). By performing tomography in vertical travel-time space, we avoid estimating mapping velocity, instead concentrating on focusing velocity. By introducing anisotropic preconditioning oriented along bedding planes, we can quickly guide the inversion towards a geologically reasonable model. We illustrate the benefits of our tomography method by comparing it to more traditional methods on a synthetic anticline model. In addition, we demonstrate the method's ability to improve the velocity estimate, and the resulting migrated image of a real 2-D dataset.

INTRODUCTION

Tomography is inherently non-linear, therefore a standard technique is to linearize the problem by assuming a stationary ray field (Stork and Clayton, 1991). Unfortunately, we must still deal with the coupled relationship between reflector position and velocity (Al-Chalabi, 1997; Tieman, 1995). As a result, the back projection operator must attempt to handle both repositioning of the reflector *and* updating the velocity model (van Trier, 1990) . The resulting back projection operator is sensitive to our current guess at velocity and reflector position.

In addition to non-linearity, tomography problems are often under-determined. To create more geologically feasible velocity models and to speed up convergence, Michelena (1991) suggested using varying sized grid cells. Unfortunately, such a parameterization is prone to error when the wrong size blocks are chosen (Delprat-Jannaud and Lailly, 1992). Other authors have suggested locally clustering grid cells (Carrion, 1991) or characterizing the velocity model as a series of layers (Kosloff et al., 1996). These methods are also susceptible to errors when the wrong parameterization is chosen. An attractive alternative approach is to add an additional model regularization term to our objective function (Toldi, 1985). In theory, this regularization term should be the inverse model covariance matrix (Tarantola,

[1]**email:** bob@sep.stanford.edu, biondo@sep.Stanford.EDU

1987). The question is how to obtain an estimate of the model covariance matrix. The obvious answer is through *a priori* information sources such a geologist's structural model of the area, well log information, or preliminary stack or migration results. Incorporating these varied information sources into our objective function has always been problematic. For years, geostatisticians have successfully combined these mixed types of information to produce variograms (Issaks and Srivastava, 1989). Unfortunately, the geostatistical approach does not easily fit within a standard global tomography problem. In this paper we follow the course outlined in Clapp and Biondi (1998) to address both the velocity-depth ambiguity and the problem of adding geologic constraints. We formulate our tomography problem in vertical travel-time (τ) coordinates rather than depth. In this coordinate system, reflectors are significantly less sensitive to velocity (Biondi et al., 1997) and the resulting back projection operator is less sensitive to the background velocity model (Clapp and Biondi, 1999). We make the assumption that velocity follows geologic dip or some other known trend. We then approximate the model covariance matrix by creating small, plane-wave annihilation filters (Claerbout, 1992b), or *steering filters* oriented along geologic dip (Clapp et al., 1997, 1999). To speed up convergence, we reformulate our regularization problem to a preconditioned problem (Claerbout, 1998) using the helix transform and polynomial division (Claerbout, 1998b).

We create a synthetic anticline velocity model and compare the inversion result using a symmetric regularization operator in depth, steering filter in depth, and finally steering filter in vertical travel time space. We study the speed and quality of our tomographic estimate using two different synthetic models. We conclude with some preliminary tests on a 2-D marine dataset with gas hydrates. Preliminary migration results are encouraging.

THEORY

Following the method described in Clapp (1998), we began by linearizing the tomography problem around an initial guess at our slowness model $\mathbf{s_0}$. We assumed ray stationarity and described the change in travel time ($\Delta\mathbf{t}$) as being linearly related to our change in slowness ($\Delta\mathbf{s}$):

$$\Delta\mathbf{t} \approx \mathbf{T_z}\Delta\mathbf{s}. \tag{1}$$

$\mathbf{T_z}$ is composed of two portions. The first, $\mathbf{T_{z,ray}}$ simply applies

$$\delta t = \tilde{l}\delta s, \tag{2}$$

or that the change in the travel time is (δt) is equal to change in slowness (δs) times length of the ray of the ray segment ($\tilde{l}$) of the ray connecting the source, reflector, and the receiver. The second component, $\mathbf{T_{z,ref}}$, can be thought of as a chain of two operators: the first maps our change in slowness ($\Delta\mathbf{s}$) into reflector movement, the second maps the reflector movement into our change in travel times ($\Delta\mathbf{t}$) (van Trier, 1990). This second term amounts to performing residual migration and can be done by back projecting a ray located at the reflection point perpendicular to the reflector (Stork, 1994), Figure 1. Taking both components into account our tomography fitting goal becomes

$$\Delta\mathbf{t} \approx (\mathbf{T_{z,ray}} + \mathbf{T_{z,ref}})\Delta\mathbf{s}. \tag{3}$$

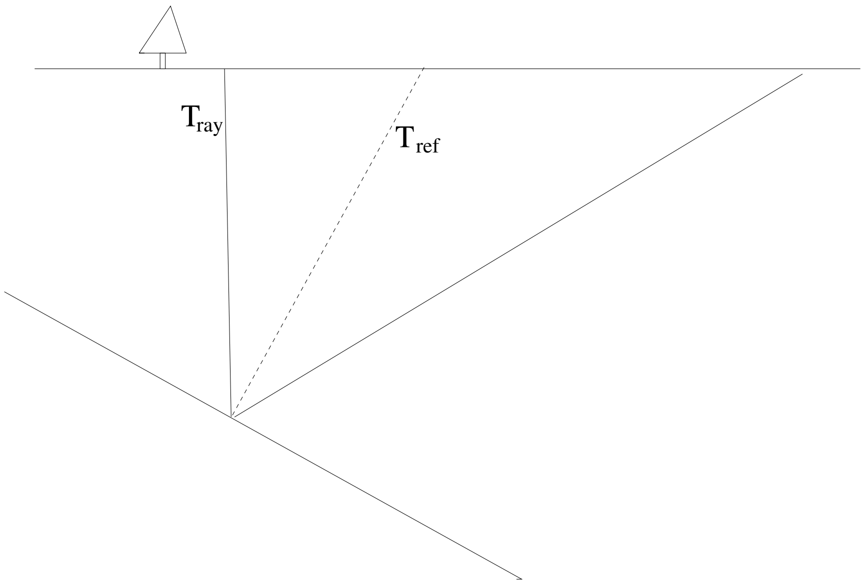

Figure 1: The two portions of the back projection operator. $\mathbf{T_{z,ray}}$ is the pair of rays through $\mathbf{s_0}$ from the source to the receiver that obey Snell's law at the reflector. $\mathbf{T_{z,ref}}$ is the raypath from this reflection point to the surface. bob1-schematic [NR]

Smoothing slowness rather than change of velocity

In general, the tomography problem is under-determined and requires some type of regularization. Ideally, this regularization should be the inverse model covariance (Tarantola, 1987) but that is not readily available. In many cases we do have well logs, initial migration surfaces, or a geologist's model of the region that can at least indicate the trend that velocity should follow. Following the method described in Clapp, et al. (1999) we can build a space-varying operator composed of small plane wave annihilation filters that can smooth our velocity along this predetermined trend. The problem is that our model is not slowness, but change in slowness. To a degree, we can get around this problem by following the method similar to the one described by Bevc (1994). We start by stating our goal to smooth the slowness field:

$$\mathbf{0} \approx \mathbf{A}\mathbf{s} \tag{4}$$

where $\mathbf{A}$ is our steering filter operator. But $\mathbf{s}$ is actually $\mathbf{s_0} + \Delta\mathbf{s}$, so we can write a new regularization goal as

$$\begin{aligned} \mathbf{0} &\approx \mathbf{A}(\mathbf{s_0} + \Delta\mathbf{s}) \\ -\mathbf{A}\mathbf{s_0} &\approx \mathbf{A}\Delta\mathbf{s}. \end{aligned} \tag{5}$$

A problem with this method is where the adjoint of our modeling operator ($\mathbf{T_z^{'}}$) does not contribute at all to the model we can introduce artifacts. Our best solution to date for this problem is to introduce a smooth masking operator that tapers off to zero in locations unaffected by $\mathbf{T_z^{'}}$.

Preconditioning

The proposed regularized tomography problem still has the problem of slow convergence. By reformulating the problem in helix space (Claerbout, 1998b), we can take advantage of 1-D theory to change our regularized problem into a preconditioned one. We start by defining a new variable $\mathbf{p}$:

$$\mathbf{p} = \mathbf{A}\Delta\mathbf{s}. \tag{6}$$

By applying polynomial division to our steering filters, we can create $\mathbf{A}^{-1}$ which becomes a smoothing operator. We can then rewrite our fitting goals as

$$\begin{aligned} \Delta\mathbf{t} &\approx (\mathbf{T}_{\mathbf{z,ray}} + \mathbf{T}_{\mathbf{z,ref}})\mathbf{A}^{-1}\mathbf{p} \\ -\mathbf{A}\mathbf{s_0} &\approx \epsilon\mathbf{p}. \end{aligned} \tag{7}$$

Tau tomography

In depth tomography we must constantly deal with the depth-velocity ambiguity problem. Put another way, we are simultaneously trying to estimate both a focusing (S_f) and a mapping (S_m) slowness. Biondi et al.(1997) showed that by mapping (z, x) into (τ, x) through

$$\tau(z, x) = \int_0^z 2S(z', x)\delta z' \tag{8}$$

we can write a **focusing eikonal** equation which only indirectly depends on the mapping velocity

$$4\left(\frac{\partial t(\tau, x)}{\partial \tau}\right) + S_f(\tau, x)^{-2}\left(\frac{\partial t(\tau, x)}{\partial x} + \sigma_m(\tau, x)\frac{\partial t(\tau, x)}{\partial \tau}\right)^2 = 1 \tag{9}$$

where σ_m is the differential mapping operator defined as

$$\sigma_m(\tau, x) = \int_0^\tau S_m^{-1}(\tau', x)\frac{\partial}{\partial x}S_f(\tau', x)\delta\tau'. \tag{10}$$

From this eikonal equation we can derive a new relation for the change in travel time due to a change in the focusing velocity:

$$\delta t = \left(\frac{\tilde{\delta x}^2}{\tilde{l}}\right)\delta s - \left(\tilde{\delta x}(\tilde{\delta\tau} - \tilde{\delta x}\tilde{\sigma_0}(x, \tau))\right)\delta\sigma \tag{11}$$

where $\tilde{\delta x}$ and $\tilde{\delta\tau}$ are the change in x and τ position of the ray segment, $\tilde{\sigma_0}(x, \tau)$ is the differential mapping factor of our initial slowness model at the ray location, and $\delta\sigma$ is defined as

$$\delta\sigma(\tau, x) = \frac{\sigma_0(\tau, x)}{s_0(\tau, x)}\delta s(\tau, x) - 2s_0(\tau, x)\frac{\delta(\delta z(\tau, z))}{\delta x} \tag{12}$$

where

$$\delta z(\tau, z) = \int_0^\tau \frac{\delta s(\tau', x)}{2s_0^2(\tau', x)}\delta\tau. \tag{13}$$

We now have a way to back project travel time errors and can write a new set of fitting goals,

$$\begin{aligned} \mathbf{\Delta t} &\approx (\mathbf{T}_{\tau,\mathbf{ray}} + \mathbf{T}_{\tau,\mathbf{ref}})\mathbf{A}^{-1}\mathbf{p} \\ -\mathbf{A}\mathbf{s_0} &\approx \epsilon\mathbf{p} \end{aligned} \tag{14}$$

where $\mathbf{T}_{\tau,\mathbf{ray}}$ and $\mathbf{T}_{\tau,\mathbf{ref}}$ use (11) rather than (2) to back project.

SYNTHETIC TESTS

To test the effectiveness of the method we create a simple anticline synthetic velocity model, Figure 2. We simulated six reflectors, one on top, four in the anticline, and a basement reflector. We calculated travel times to all the reflectors for an offset range of 4 kms. These travel times represent our 'recorded travel times'. For our initial model we created a v(z) model by taking the lateral average of the velocity field, Figure 2. From this initial model

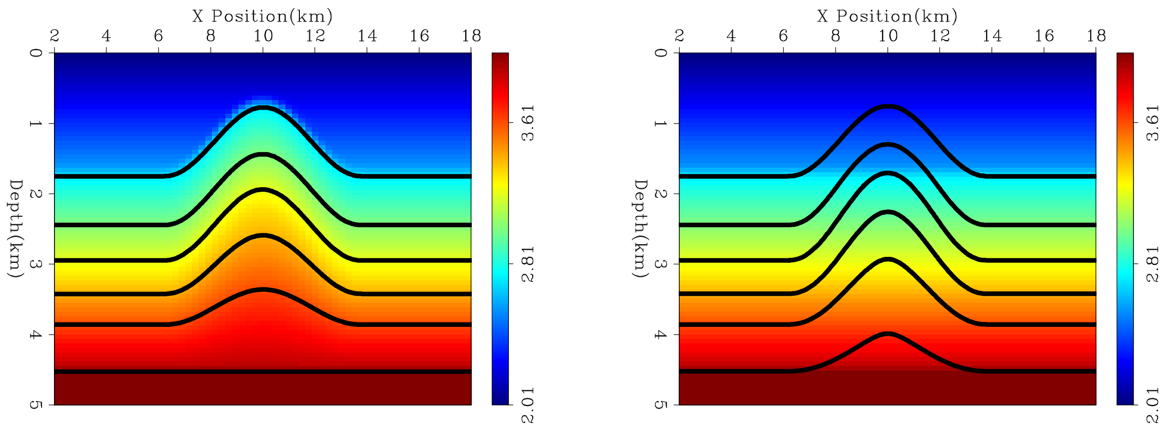

Figure 2: Left panel is our synthetic model superimposed by the six reflectors. The right panel is our starting guess for our velocity function and the map migrated reflector position using this initial velocity estimate. bob1-model [CR]

we attempted to invert the velocity function by three progressively advanced methods:

Depth-Standard : Inverted for a depth model, using an inverse Laplacian preconditioner (Claerbout, 1998b) for $\mathbf{A}^{-1}$ in our depth fitting goals (7)

Depth-Steering : Inverting for a depth model, using a steering filter operator for our preconditioner in our depth fitting goals (7)

Tau-Steering : Inverting for a tau model, using a steering filter operator for our preconditioner in tau fitting goals (14)

Figure 3 shows the result of one non-linear iteration for all three inversions schemes. All three methods were able to recover the dome shape after one iteration. When using a Laplacian smoother the velocity increase is spread too far both laterally and vertically. As a result, the bottom reflector is located too deep throughout the model. When using steering filters we still have a significant velocity-depth ambiguity problem, but we have done a little better job position the bottom reflector. In the case of tau tomography with steering filters we have done almost a perfect job after a single iteration. We have not perfectly recovered the lower portion of the anticline structure but we have almost completely flattened the bottom reflector. To see if, and how fast, we could converge to the correct solution in depth

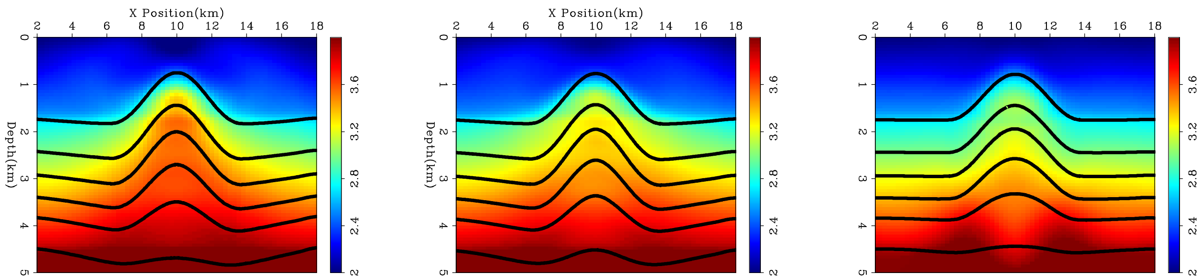

Figure 3: Left panel is Depth-Standard, middle is Depth-Steering, right is Tau-Steering. All after 1 non-linear iteration. bob1-model1-iter1 [CR]

we performed several more non-linear iterations. As Figure 4 shows we did a decent job recovering the anticline with all three methods. In this case, where the model is fairly simple and we have good travel time coverage, the big advantage seems to be speed. We got a high quality result with steering filter tau tomography in a single iteration, while it took three with steering filter depth tomography, and four when using the Laplacian and depth tomography. The smoothness of the anticline was well suited for the Laplacian so we decided on a slightly more difficult challenge that could better differentiate between a Laplacian and steering filter regularization. Our new model keeps the same basic shape for the model but adds a low velocity layer within the anticline. Figure 5 shows the correct, initial, and the result of 4 iterations using both the Laplacian and steering filters to precondition the problem. After 4 iterations the steering filters have done a much better job recovering the low velocity layer.

TEST ON REAL DATA

We next decided to test the method on real data. For this initial test we decided to work with a relatively clean data which still had some residual move-out in the common reflection point (CRP) gathers. The data is from the Blake Outer Ridge as was used by Ecker(1998) to characterize methane hydrate structures. For our initial velocity model we used Ecker's Dix (1955) derived model, Figure 6. Our general philosophy was to limit human time as much as possible. Therefore we chose to do tau migration (Alkhalifah, 1998) using a generic Kirchhoff package(Biondi, 1998). By using tau rather than depth migration, we were quickly able to compare CRPs from iteration to iteration and it allowed us to pick reflector positions only once. After performing the migration we picked six reflectors, Figure 7. We picked the sea floor, a strong reflector above the bottom simulating reflector (BSR), the BSR itself, the flat reflector below the BSR, and two deeper reflectors. Rather than pick move-out differences we decided to create residual semblance panels at each

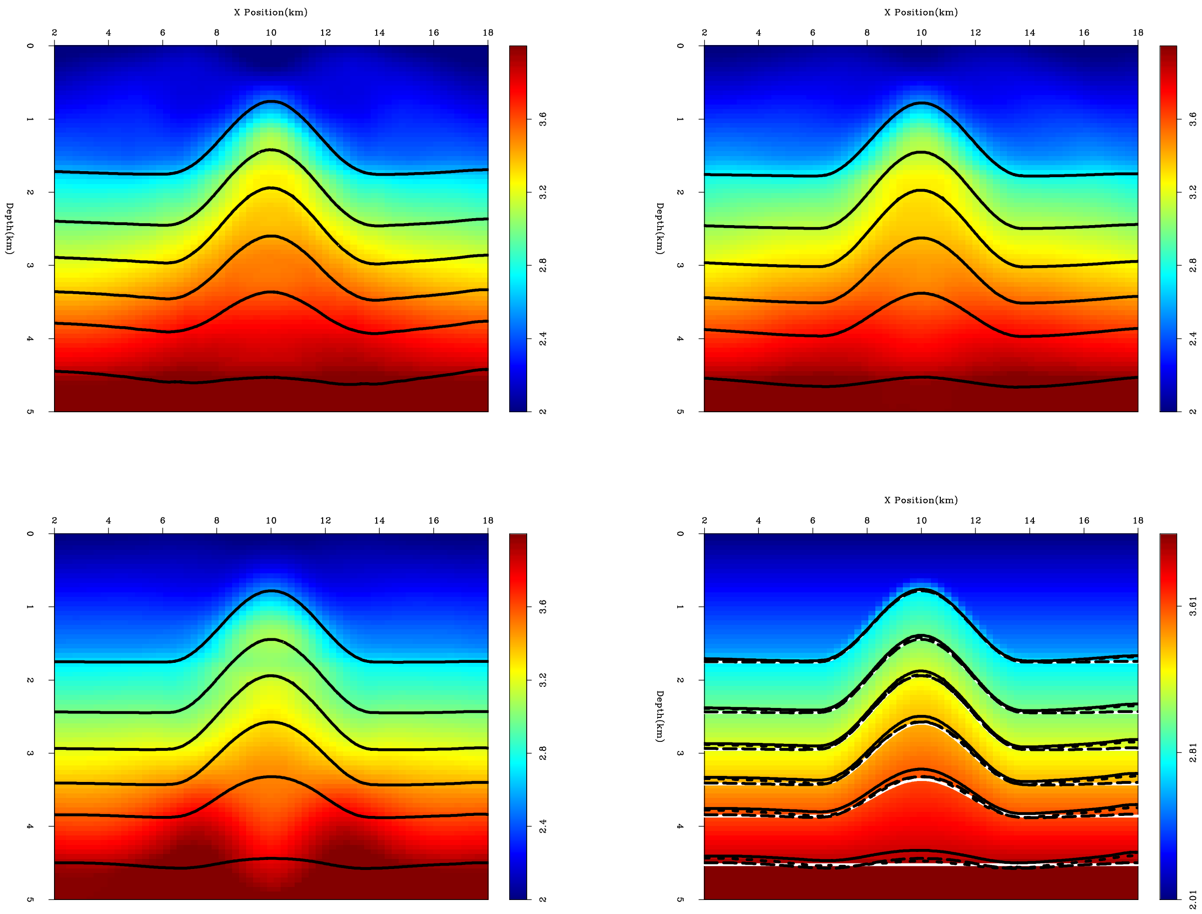

Figure 4: Top-left: Depth-Standard, after 4 non-linear iterations; top-right: Depth-Steering after 3 iterations; bottom-left: Tau-steering after 1 iteration; and bottom-right: a comparison of the reflector positions using all 3 methods. The solid, white line is correct reflector position, the small dashes represent Tau-Steering: large-dashes:Depth-Steering; and the solid black line is Depth-Standard. bob1-model1-best [CR]

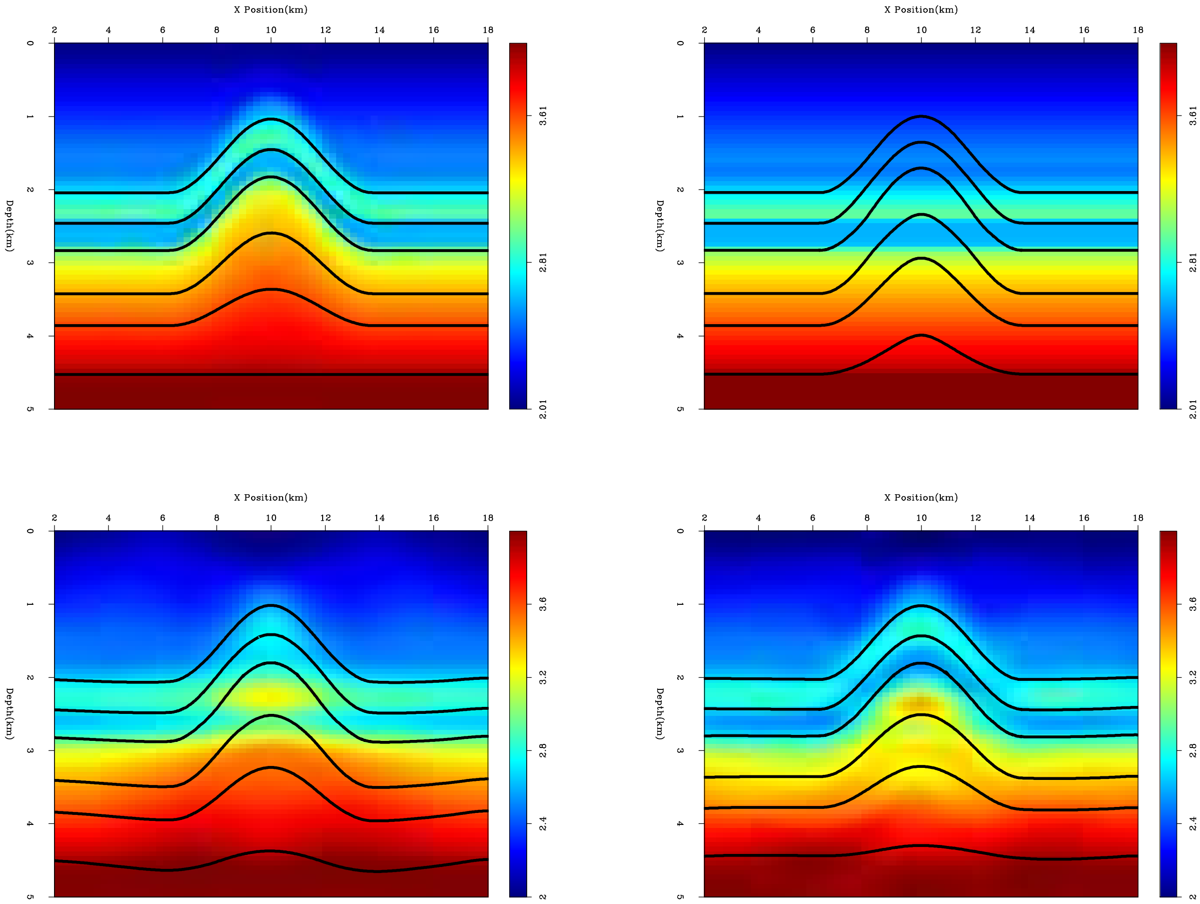

Figure 5: Top, left Our new model with a low velocity layer within the anticline; top-right, our starting model; bottom-left, Depth-Standard after 4 iterations; bottom-right Depth-Steering after 4 iterations. $\boxed{\text{bob1-model2}}$ [CR]

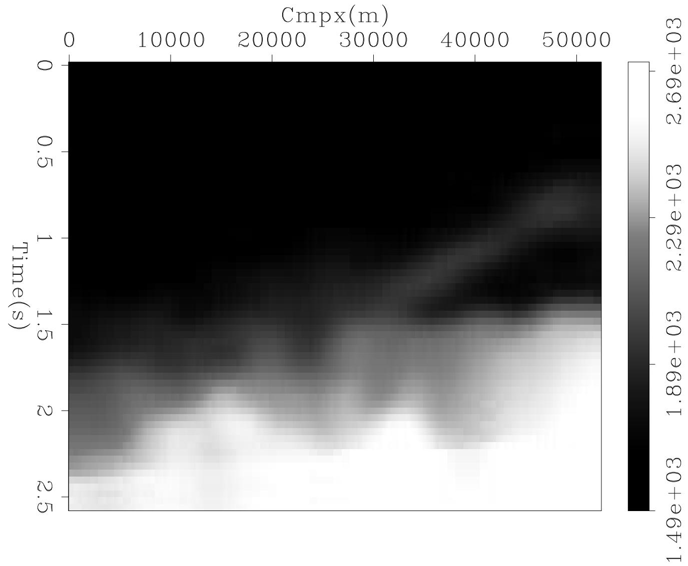

Figure 6: Initial velocity model in depth. Note the low velocity zone caused by the gas hydrate starting at approximately 32000 kms and extending to the end of the section. bob1-christine-vel0 [NR]

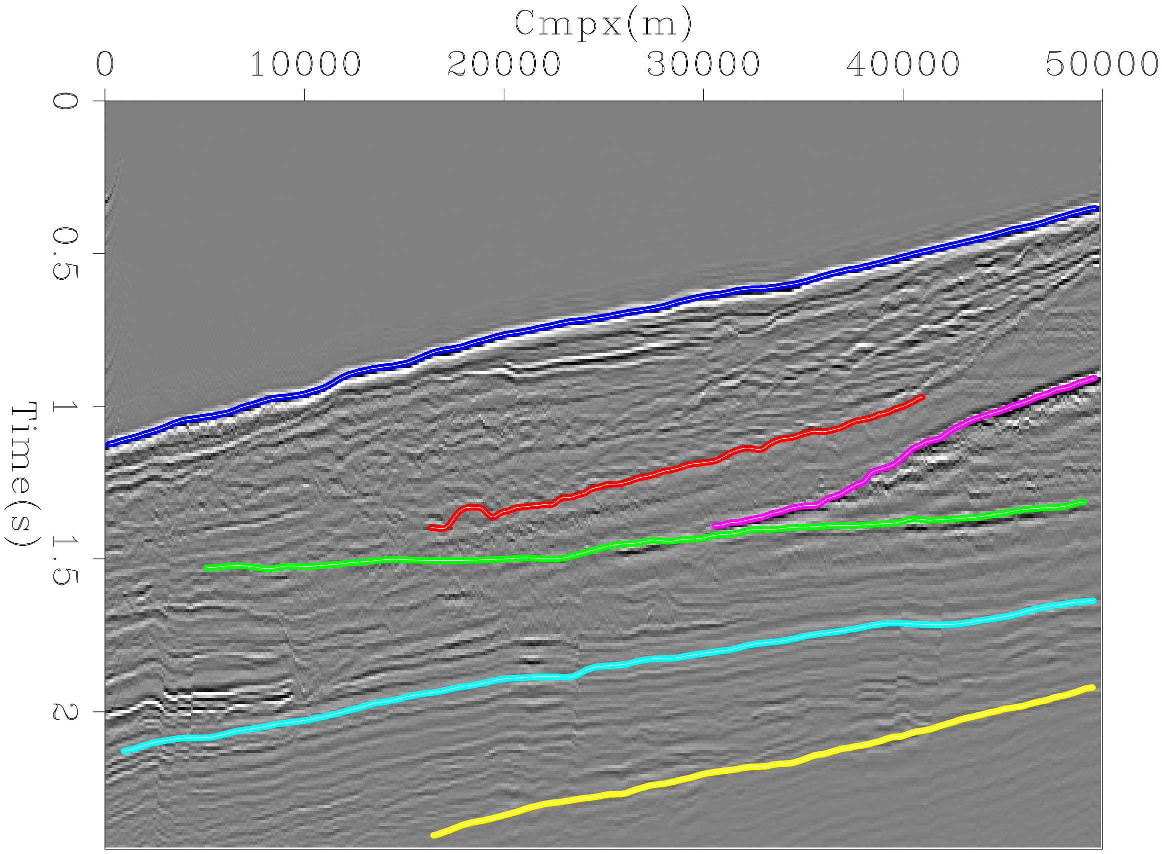

Figure 7: Initial stack overlaid by reflectors picked for tomography. bob1-stack [CR]

reflector location, Figure 8. The panels indicate that there is significant residual curvature, especially where the BSR meets the lower reflector. From these semblance panels we picked smooth curves at approximately the maximum semblance at each reflector. To check to see if a single parameter adequately described the move-outs we back projected the picked semblance into our CRP gathers. Figure 9 shows that the semblance picks did a fairly good job describing the move-out. We used our picked reflectors to construct our steering

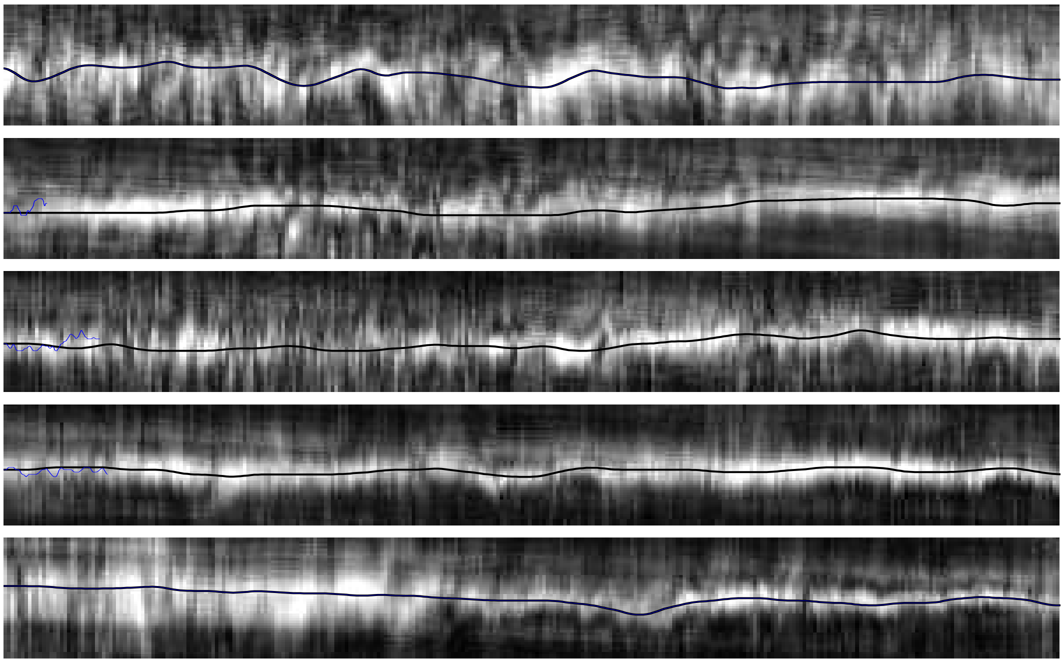

Figure 8: Residual semblance panels for the bottom 5 reflectors. The black line in each panel represents the picked maximum. bob1-sem-vel0 [CR]

filters and then applied our tau tomography fitting goals (14). Generally, we have increased velocity, Figure 10, but the changes still keep velocity following reflector dip. The next step is to see if our new velocity model flattens our CRP gathers and improves the focusing of the data. Figures 11 and 12 indicate that we have accomplished both of these goals. Figure 9 shows that all of our reflectors are significantly flatter, with only significant curvature left along the BSR. Figure 12 shows a much more continuous BSR reflection along with overall improved focusing of the section above and below.

CONCLUSIONS

By performing tomography in tau space we are able to quickly converge to geologically realistic velocity models. The results on synthetics indicate that the method when velocity is not the smooth function that the a Laplacian regularize will attempt to create. Early tests on field data are encouraging.

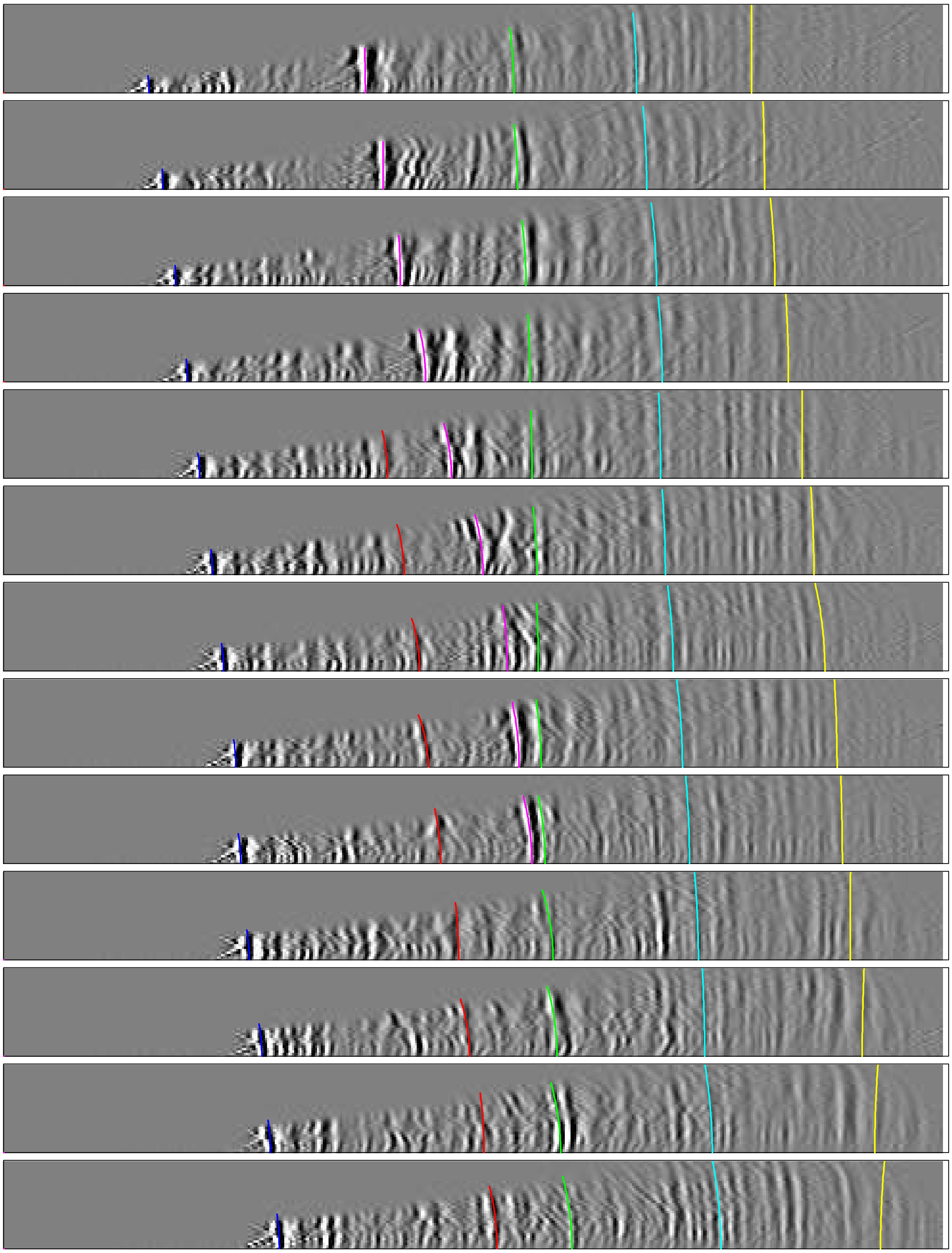

Figure 9: Common reflection point gathers from every 2000 meters starting from 28000. The lines are the result of mapping back the picked residual slowness values. Note how the curves do an excellent job matching the actual reflector move-out. bob1-overlay.vel0 [CR]

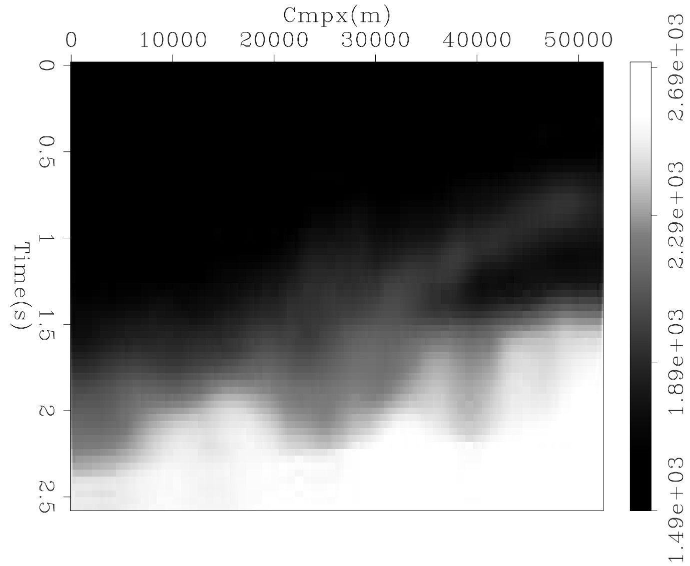

Figure 10: The velocity after 1 iteration of tau-steering tomography bob1-christine-vel1 [CR]

REFERENCES

Al-Chalabi, M., 1997, Parameter nonuniqueness in velocity versus depth functions: Geophysics, **62**, no. 03, 970–979.

Alkhalifah, T., 1998, Prestack Kirchhoff time migration for complex media: SEP–**97**, 45–60.

Bevc, D., 1994, Datuming velocity from traveltime tomography: SEP–**82**, 145–164.

Biondi, B., Fomel, S., and Alkhalifah, T., 1997, “focusing” eikonal equation and global tomography: SEP–**95**, 61–76.

Biondi, B., 1998, Genkir3D: A toolkit for Kirchhoff imaging: SEP–**97**, 371–402.

Carrion, P., 1991, Dual tomography for imaging complex structures: Geophysics, **56**, no. 9, 1395–1404.

Claerbout, J. F., 1992, Earth Soundings Analysis: Processing versus Inversion: Blackwell Scientific Publications.

Claerbout, J. Geophysical Estimation by Example: Environmental soundings image enhancement:. http://sepwww.stanford.edu/sep/prof/, 1998.

Claerbout, J., 1998b, Multidimensional recursive filters via a helix: SEP–**97**, 319–336.

Claerbout, J. F., 1998c, Multi-dimensional recursive filtering via the helix: Geophysics, **63**, no. 5, 1532–1541.

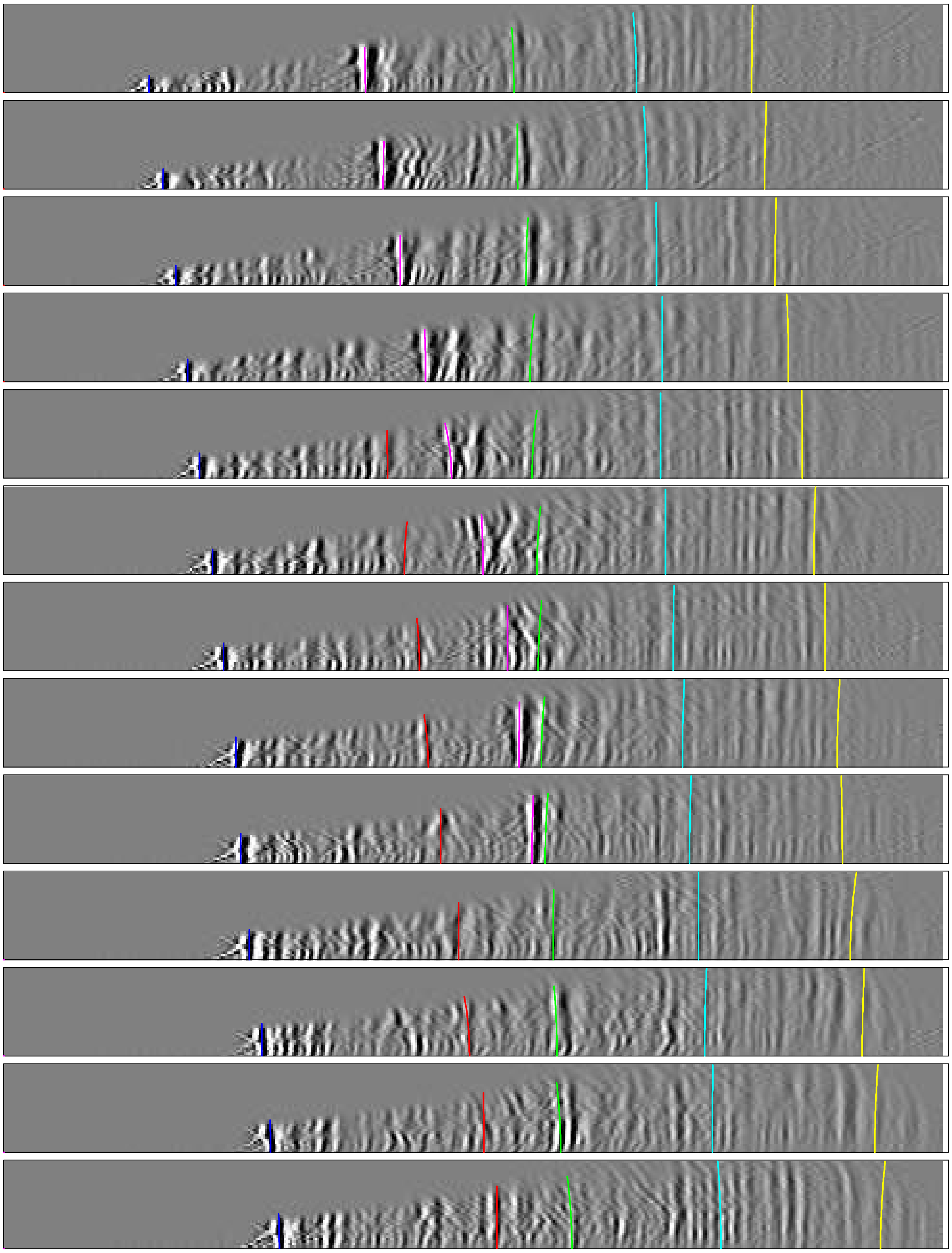

Figure 11: CRP gather from 24000-48000 meters. Note how they are considerably flatter than Figure 9. bob1-overlay.vel1 [CR]

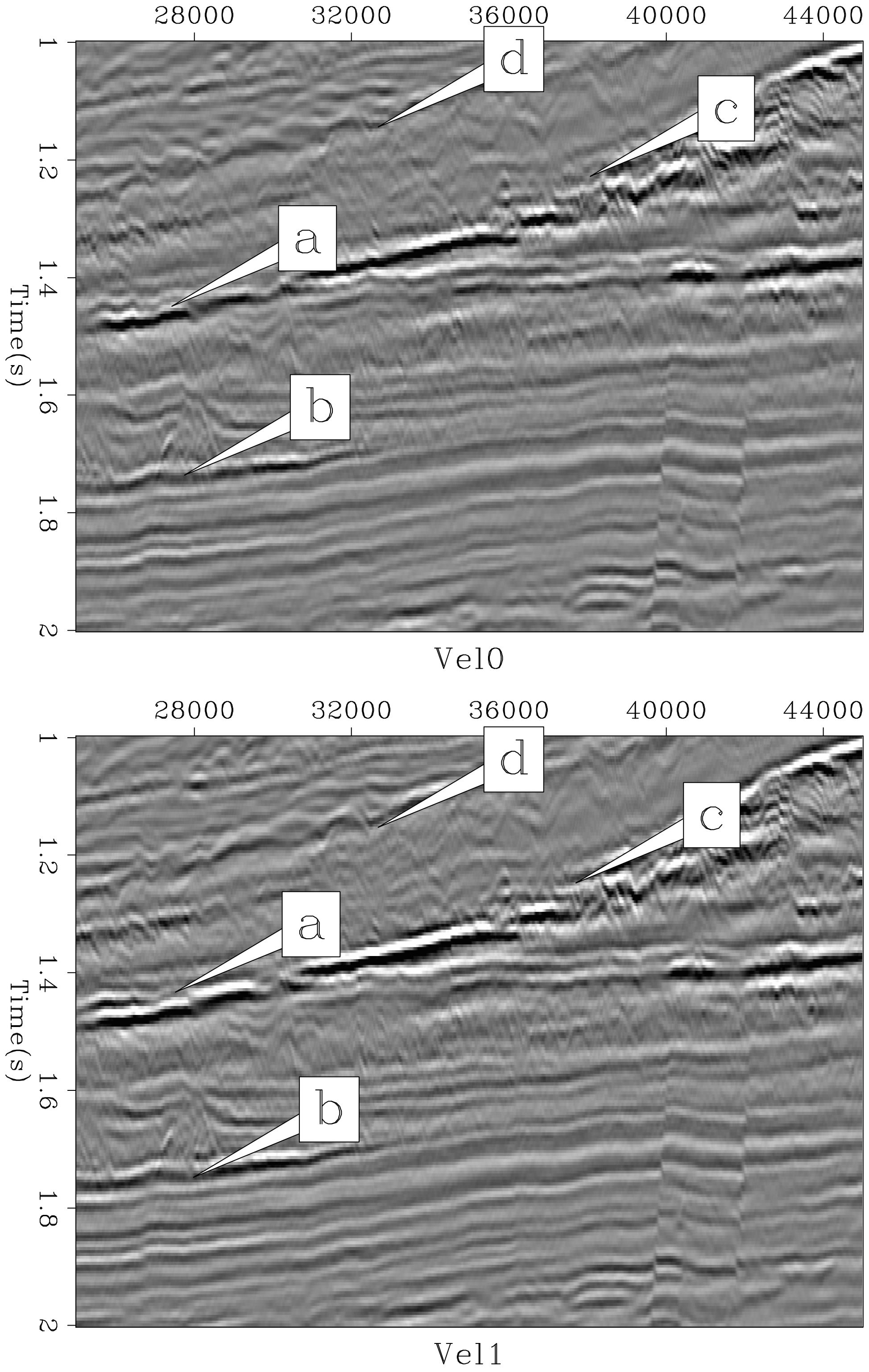

Figure 12: The stack using our initial velocity and the velocity after 1 iteration of tau steering tomography. Note how the reflectors are generally better focused at a, b, c, and d. bob1-stack-comp [CR]

Clapp, R. G., and Biondi, B. L., 1998, Regularizing time tomography with steering filters: SEP–**97**, 137–146.

Clapp, R. G., and Biondi, B., 1999, Why tau tomography is better than depth tomography: SEP–**100**, 51–58.

Clapp, R. G., Fomel, S., and Claerbout, J., 1997, Solution steering with space-variant filters: SEP–**95**, 27–42.

Clapp, R. G., Fomel, S., Crawley, S., and Claerbout, J. F., 1999, Directional smoothing of non-stationary filters: SEP–**100**, 197–210.

Delprat-Jannaud, F., and Lailly, P., 1992, What information on the earth model do reflection travel times provide?: J. Geophysical Research, **97**, 19827–19844.

Dix, C. H., 1955, Seismic velocities from surface measurements: Geophysics, **20**, no. 01, 68–86.

Ecker, C., 1998, Seismic characterization of methane hydrate structures: SEP–**96**.

Issaks, E. H., and Srivastava, R. M., 1989, An Introduction to Applied Geostatistics: Oxford University Press.

Kosloff, D., Sherwood, J., Koren, Z., Machet, E., and Falkovitz, Y., 1996, Velocity and interface depth determination by tomography of depth migrated gathers: 61, **5**, no. 1511-1523.

Michelena, R. J., and Harris, J. M., 1991, Tomographic traveltime inversion using natural pixels: Geophysics, **56**, no. 5, 635–653.

Stork, C., and Clayton, R. W., 1991, An implementation of tomographic velocity analysis: Geophysics, **56**, no. 4, 483–495.

Stork, C., 1994, Demonstration of mva tomography with controls and constraints for determining an accurate velocity model for prestack depth migration: 64th Annual Internat. Mtg., Soc. Expl. Geophys., Expanded Abstracts, 1338–1342.

Tarantola, A., 1987, Inverse problem theory: Elsevier.

Tieman, H. J., 1995, Migration velocity analysis: Accounting for the effects of lateral velocity variations: Geophysics, **60**, no. 01, 164–175.

Toldi, J., 1985, Velocity analysis without picking: SEP–**43**.

van Trier, J., 1990, Tomographic determination of structural velocities from depth migrated seismic data: Ph.D. thesis, Stanford University.